SUPPLEMENTAL FIGURES

Figure S1:

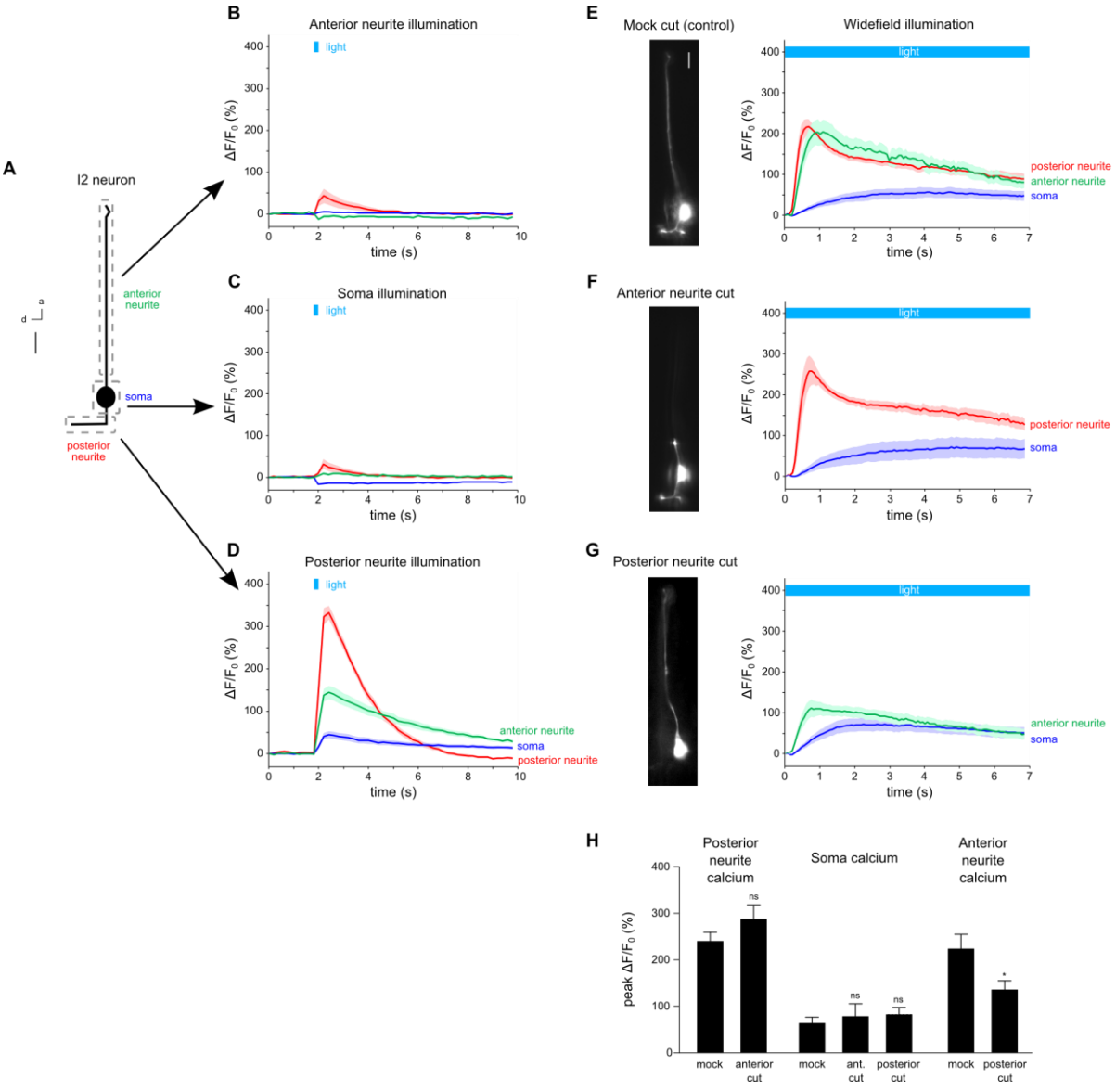

Figure S1, related to Figure 1. Exposing different compartments of I2 to light differentially triggers a calcium response.

(A) Diagram of an I2 neuron indicating regions exposed to spatially-restricted illumination (rastered 488 nm). Dashed gray boxes indicate three areas of illumination. d = dorsal, a = anterior, scale bar = 5 µm.
(B-G) Red trace is the response of the posterior neurite, blue is the response of the soma, and green is the response of the anterior neurite of I2.
(B) I2 responded weakly after anterior neurite illumination. n = 11 neurons.

(C) I2 responded weakly after soma illumination. n = 11.
(D) I2 responded strongly after posterior neurite illumination. n = 11. The small declines in signal in (B**)** and (C) were a consequence of anterior neurite and soma bleaching, respectively.
(E) An intact I2 neuron responded normally to light (control). n = 13.
(F) An I2 neuron with a cut anterior neurite responded normally to light. n = 7.
(G) An I2 neuron with a cut posterior neurite responded less to light than did an intact I2 neuron. n = 15.
(H) Quantification of the calcium response in different compartments after ablating the anterior or posterior neurite. Cutting the posterior neurite reduced the response in the anterior neurite but did not eliminate it.

Error bars and shading around traces indicate s.e.m. * $p < 0.05$, ns = not significant at $p < 0.05$, t-test compared to mock control.

Figure S2:

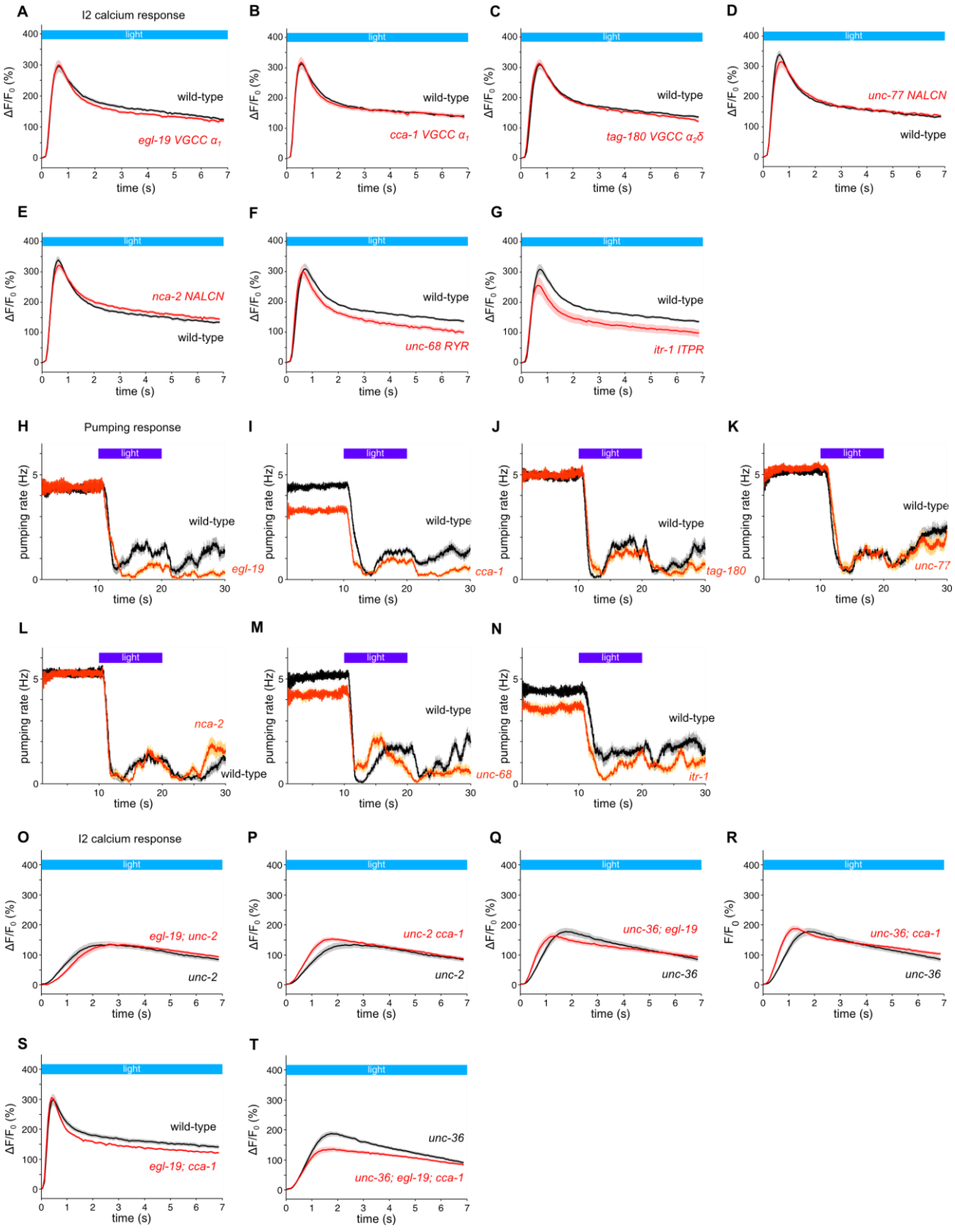
A
I2 calcium response
light
wild-type
egl-19 VGCC α1
ΔF/F0 (%)
time (s)
B
cca-1 VGCC α1
C
tag-180 VGCC α2δ
D
unc-77 NALCN
E
nca-2 NALCN
F
unc-68 RYR
G
itr-1 ITPR
H
Pumping response
pumping rate (Hz)
egl-19
I
cca-1
J
tag-180
K
unc-77
L
nca-2
M
unc-68
N
itr-1
O
egl-19; unc-2
unc-2
P
unc-2 cca-1
Q
unc-36; egl-19
unc-36
R
F/F0 (%)
unc-36; cca-1
S
egl-19; cca-1
T
unc-36; egl-19; cca-1

Figure S2, related to Figure 2. Calcium channel mutants that exhibited a normal I2 calcium response to light, a normal acute pumping response, and a failure to enhance the I2 response defect of *unc-2* and *unc-36* mutants.

(A) *egl-19(n582)* mutants showed a normal calcium response in I2. n = 20 neurons.
(B) *cca-1(ad1650)* mutants showed a normal calcium response in I2. n = 21.
(C) *tag-180(ok779)* mutants showed a normal calcium response in I2. n = 21.
(D) *unc-77(gk9)* mutants showed a normal calcium response in I2. n = 22.
(E) *nca-2(gk5)* mutants showed a normal calcium response in I2. n = 22.
(F) *unc-68(e540)* mutants showed a normal calcium response in I2. n = 22.
(G) *itr-1(sa73)* mutants showed a normal calcium response in I2. n = 21.

(H) *egl-19(n582)* mutants showed a normal acute pumping response to light. n = 20 worms.
(I) *cca-1(ad1650)* mutants showed a normal acute pumping response to light. n = 40.
(J) *tag-180(ok779)* mutants showed a normal acute pumping response to light. n = 20.
(K) *unc-77(gk9)* mutants showed a normal acute pumping response to light. n = 20.
(L) *nca-2(gk5)* mutants showed a normal acute pumping response to light. n = 20.
(M) *unc-68(e540)* mutants exhibited normal acute response latency but were defective in acute response amplitude ($p < 0.001$, t-test). n = 20.
(N) *itr-1(sa73)* mutants were not defective in the acute pumping response to light. n = 20.

(O) *egl-19; unc-2* double mutants showed a calcium response in I2 no more defective than *unc-2* mutants. n = 20 neurons.
(P) *unc-2 cca-1* double mutants showed a calcium response in I2 no more defective than *unc-2* mutants. n = 27.
(Q) *unc-36; egl-19* double mutants showed a calcium response in I2 no more defective than *unc-36* mutants. n = 20.
(R) *unc-36; cca-1* double mutants showed a calcium response in I2 no more defective than *unc-36* mutants. n = 20.
(S) *egl-19; cca-1* double mutants showed a normal calcium response in I2. n = 21.
(T) *unc-36; egl-19; cca-1* triple mutants showed a modest reduction in the calcium response in I2 compared with *unc-36* mutants. n = 27.

(A-G, O-T) Calcium response in the posterior neurite of I2.

Shading around traces indicate s.e.m.

Figure S3:

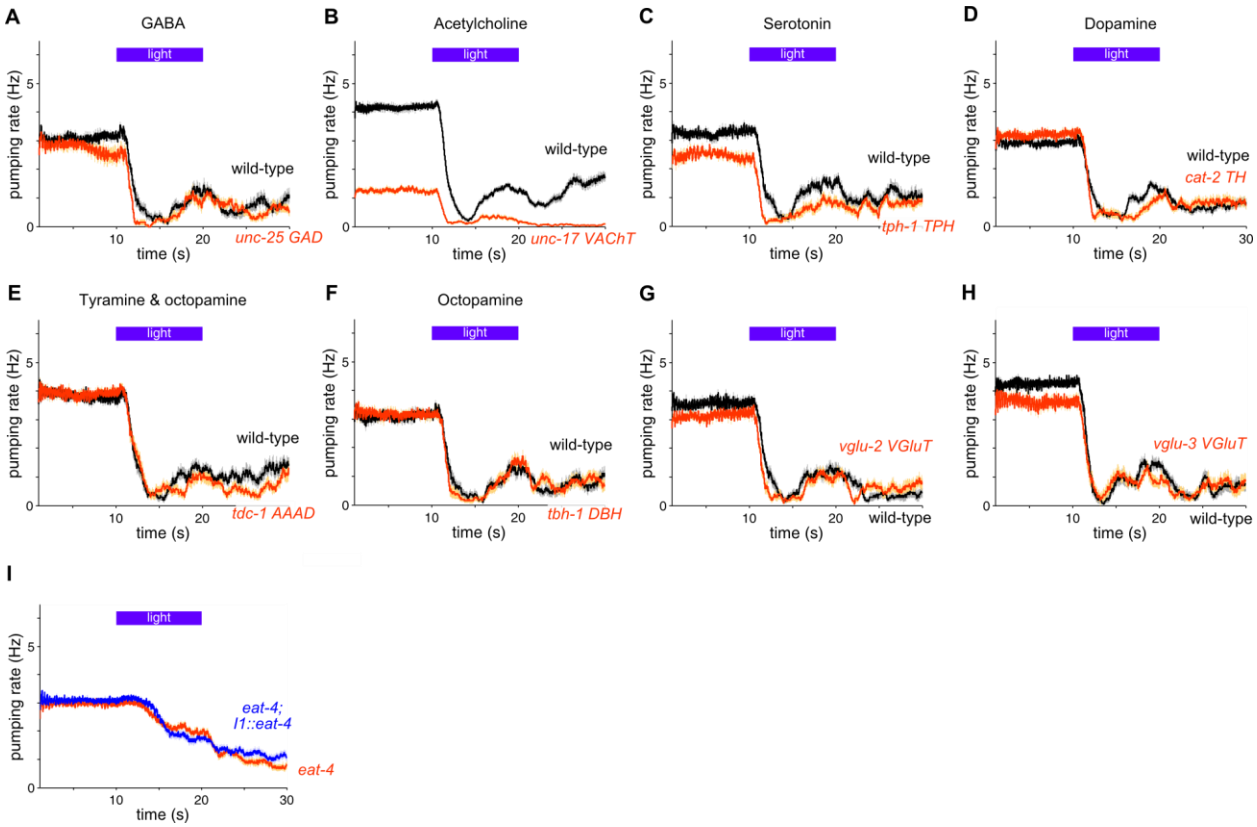

Figure S3, related to Figure 3. Neurotransmitter mutants with a normal acute response to light, and the failure of I1-specific expression of eat-4 to rescue eat-4 mutants.

(A) *unc-25(e156) GAD* mutants defective in GABA synthesis showed a normal pumping response to light. 20 °C, n = 20 worms.
(B) *unc-17(e245) VAChT* mutants defective in vesicular acetylcholine import showed a normal acute response to light. 20 and 22.5 °C, n = 80.
(C) *tph-1(n4622) TPH* mutants defective in serotonin synthesis showed a normal acute response to light. 20 °C, n = 20.
(D) *cat-2(e1112) TH* mutants defective in dopamine synthesis showed a normal pumping response to light. 20 °C, n = 40.
(E) *tdc-1(n3420) AAAD* mutants defective in tyramine and octopamine synthesis showed a normal pumping response to light. 20 °C, n = 20.
(F) *tbh-1(n3722) DBH* mutants defective in octopamine synthesis showed a normal pumping response to light. 20 °C, n = 20.
(G) *vglu-2(ok2356) VGluT* mutants defective in glutamate transport showed a normal pumping response to light. n = 20.
(H) *vglu-3(tm3390) VGluT* mutants defective in glutamate transport showed a normal pumping response to light. n = 20.

(I) I1-specific expression of *eat-4* (*gcy-10*$_{prom}$*::eat-4 cDNA::gfp*) failed to rescue the pumping response defect of *eat-4* mutants. n = 60.

Shading around traces indicate s.e.m.

Figure S4:

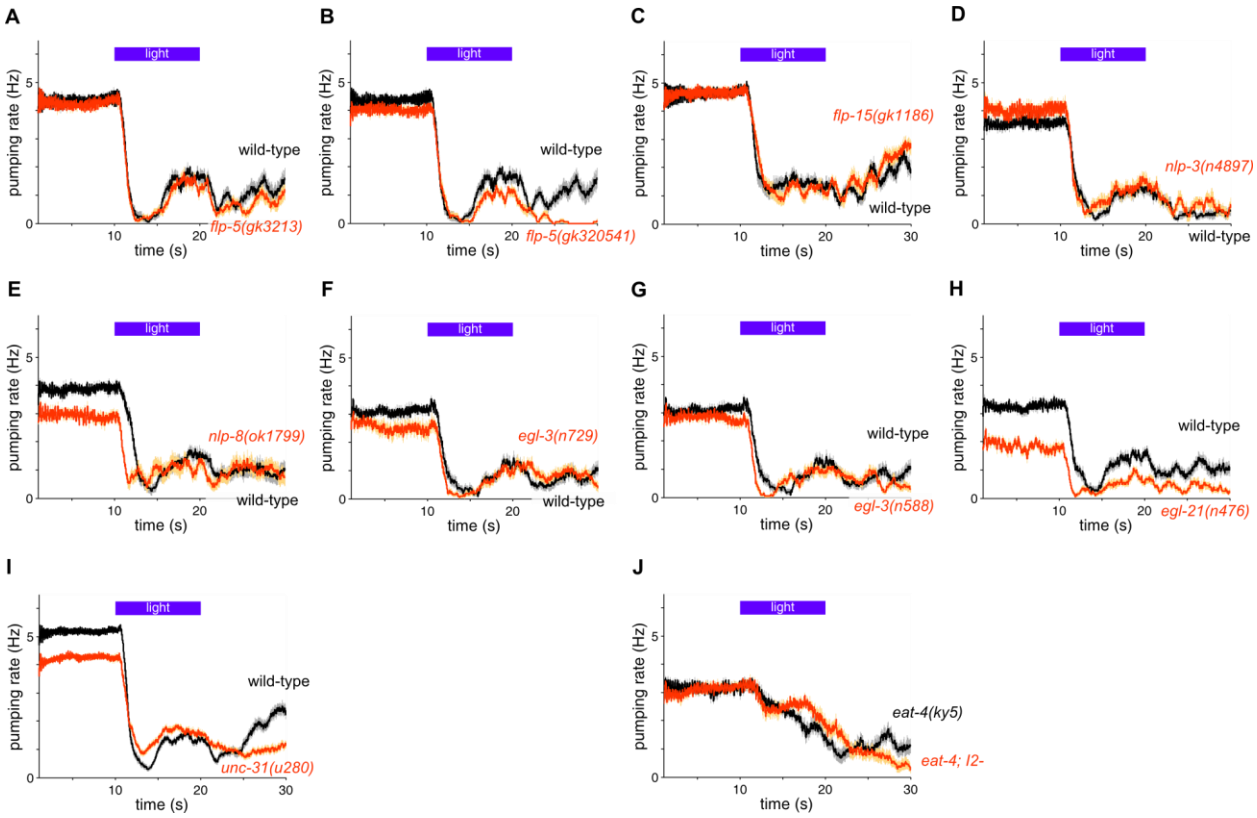

Figure S4, related to Figure 3: Mutants of neuropeptide genes expressed in I2 have a normal acute response to light, although unc-31 has a defect in the amplitude of the acute response.

(A) *flp-5(gk3213)* mutants showed a normal pumping response to light. n = 20 worms.
(B) *flp-5(gk320541)* mutants showed a normal acute pumping response to light. n = 20.
(C) *flp-15(gk1186)* mutants showed a normal pumping response to light. n = 20.
(D) *nlp-3(n4897)* mutants showed a normal pumping response to light. n = 20.
(E) *nlp-8(ok1799)* mutants showed a normal pumping response to light. n = 20.
(F) *egl-3(n729)* mutants showed a normal pumping response to light. 20 °C, n = 20.
(G) *egl-3(n588)* mutants showed a normal pumping response to light. 20 °C, n = 20.
(H) *egl-21(n476)* mutants showed a normal acute pumping response to light. 20 °C, n = 20.
(I) *unc-31(u280)* mutants showed a normal acute latency but a defective acute amplitude in response to light ($p < 0.001$, t-test). n = 60.

(J) The acute pumping response defect of *eat-4(ky5)* mutants was not further enhanced by genetic ablation of I2. n = 20.

Shading around traces indicate s.e.m.

Figure S5:

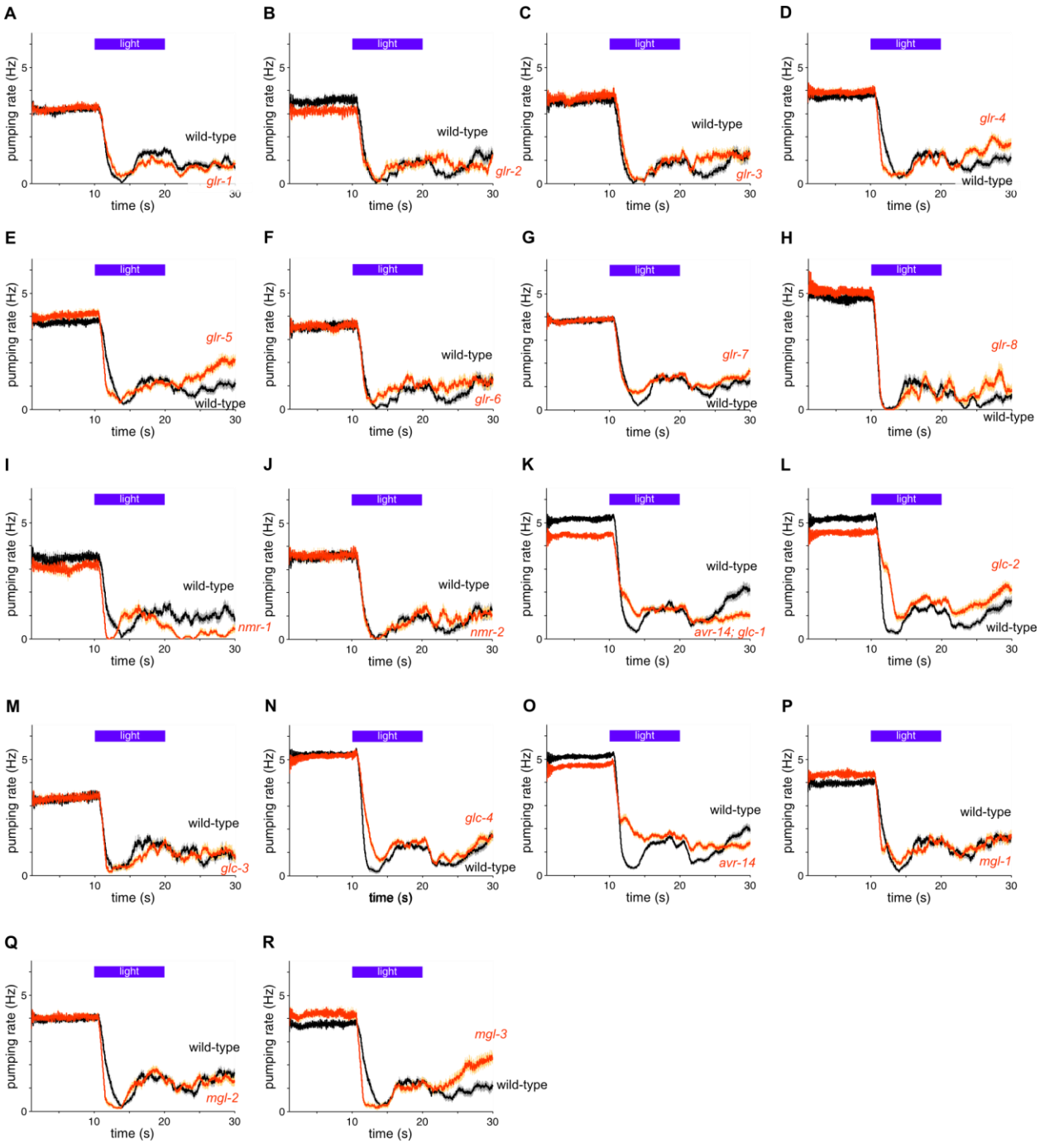

Figure S5, related to Figure 3. The pumping responses to light of glutamate receptor mutants.

(A) *glr-1(n2461)* mutants were not defective in their pumping response to light. 20 °C, n = 40 worms.

(B) *glr-2(ak10)* mutants were not defective in their pumping response to light. 20 °C, n = 20.
(C) *glr-3(ak57)* mutants were not defective in their pumping response to light. 20 °C, n = 20.
(D) *glr-4(tm3219)* mutants were not defective in their pumping response to light. n = 40.
(E) *glr-5(tm3506)* mutants were not defective in their pumping response to light. n = 40.
(F) *glr-6(ak56)* mutants were not defective in their pumping response to light. 20 °C, n = 20.
(G) *glr-7(tm2827)* mutants had a normal acute response latency and small but statistically significant reduction in acute response amplitude ($p < 0.05$, t-test). n = 60.
(H) *glr-8(gk283043)* mutants were not defective in their pumping response to light. n = 20.
(I) *nmr-1(ak4)* mutants were not defective in the acute response to light. 20 °C, n = 20.
(J) *nmr-2(ak10)* mutants were not defective in their pumping response to light. 20 °C, n = 20.
(K) *avr-14(ad1302); glc-1(pk54)* mutants had a defective amplitude in the acute response to light. Since *avr-14* single mutants also had an acute response defect of similar magnitude (see O), we attributed the defect in this strain to the *avr-14* mutation. n = 60.
(L) *glc-2(gk179)* mutants had a latency defect in the acute response to light. n = 60.
(M) *glc-3(ok321)* mutants had a normal pumping response to light. 20 °C, n = 20.
(N) *glc-4(ok212)* mutants had a latency defect in the acute response to light. n = 60.
(O) *avr-14(ad1302)* mutants had an amplitude defect in the acute response to light. n = 100.
(P) *mgl-1(tm1811)* mutants were not defective in the pumping response to light. n = 40.
(Q) *mgl-2(tm355)* mutants were not defective in the pumping response to light. n = 40.
(R) *mgl-3(tm1766)* mutants were not defective in the pumping response to light. n = 31.

Shading around traces indicate s.e.m.

Figure S6 - I2L synapses:

A Synapses from I2L (worm #1). All synapses are in the anterior neurite unless specified otherwise. Pharyngeal muscles are underlined.

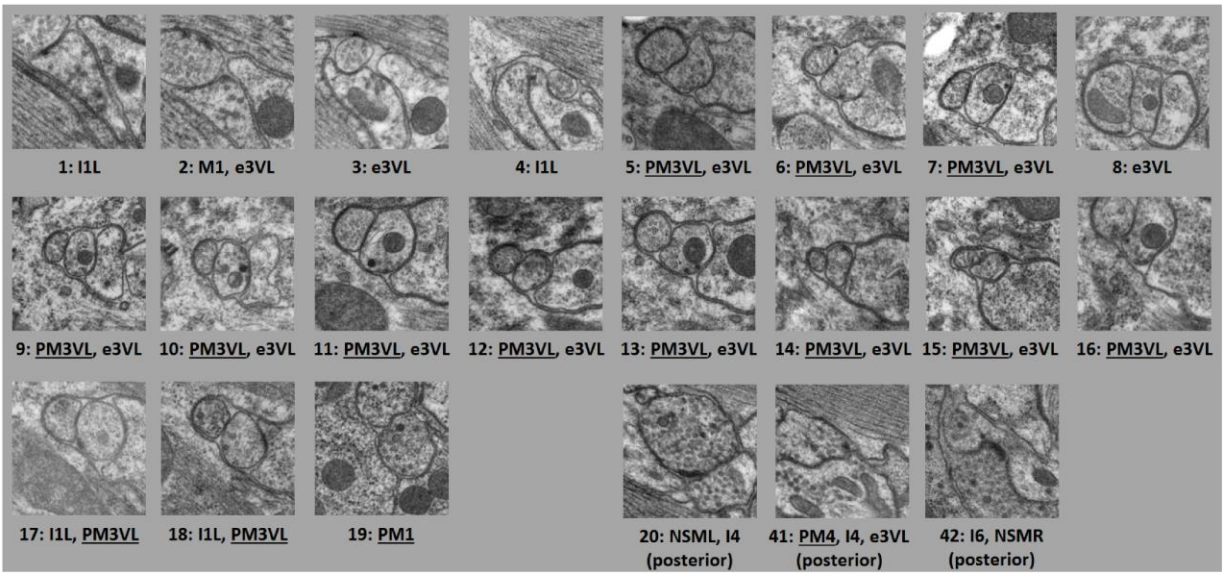

B Synapses from I2L (worm #4). All synapses are in the posterior neurite.

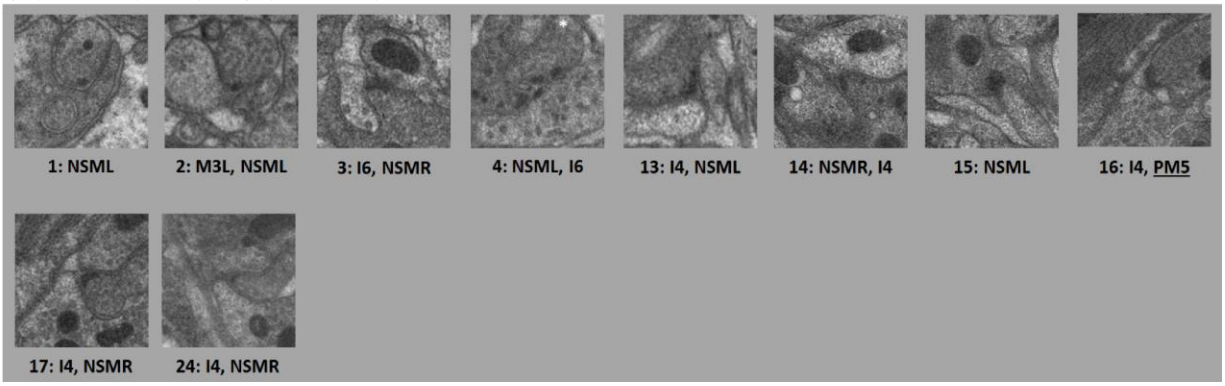

Figure S6 (cont'd) - I2R synapses:

C Synapses from I2R (worm #1). All synapses are in the anterior neurite unless specified otherwise. Pharyngeal muscles are underlined.

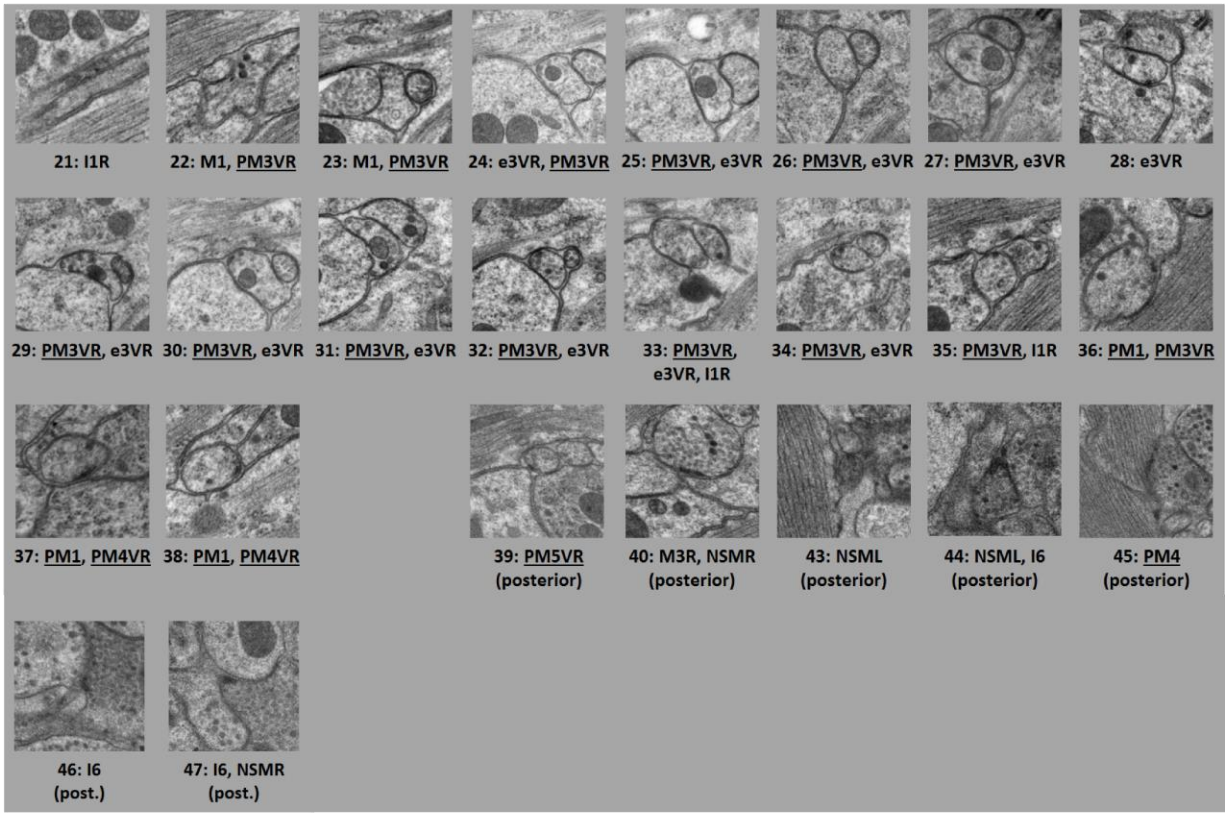

D Synapses from I2R (worm #4). All synapses are in the posterior neurite.

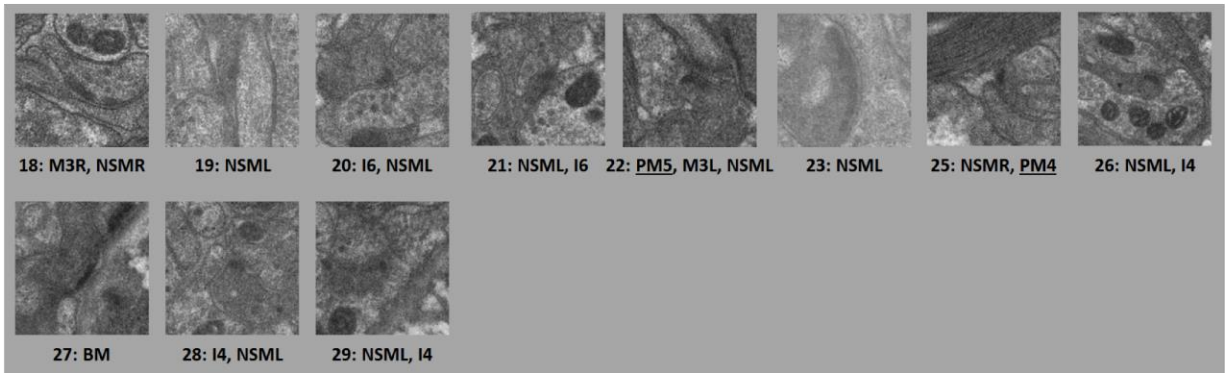

Figure S6 (cont'd) - Quantification:

E

I2L chemical synapses

	Recipient	# syn. (Albertson)	# syn. (this work)	# sections	DP vol. (nm^3)	vesicle area (nm^2)
anterior neurite	PM3VL	0	13*	133	893,560	318,307
	e3VL	0	14*	138	700,800	332,999
	I1L	0	4	23	361,000	84,068
	PM1	0	1*	9	116,200	23,192
	M1	1	1*	15	0	42,168
posterior neurite	NSMR	3 (L+R)	4*	39	8,838,700	nd
	I4	2	5*	30	6,881,600	nd
	NSML	3 (L+R)	5*	22	4,306,800	nd
	I6	1	2*	17	3,918,000	nd
	M3L	0	1*	5	798,300	nd
	PM5	0	1*	1	408.600	nd
	M1	2	0	0	0	nd
	MCL	1	0	0	0	nd

* indicates polyadic synapses were included in the synapse count

I2R chemical synapses

	Recipient	# syn. (Albertson)	# syn. (this work)	# sections	DP vol. (nm^3)	vesicle area (nm^2)
anterior neurite	PM1	0	3*	13	973,400	40,288
	PM3VR	0	14*	108	743,900	263,264
	PM4VR	0	2*	7	623,300	11,156
	e3VR	0	11*	80	405,900	180,552
	I1R	0	3*	19	106,300	36,492
	M1	1	2*	24	0	59,184
posterior neurite	NSML	3 (L+R)	8*	43	12,315,104	nd
	I6	1	2*	18	4,849,204	nd
	NSMR	3 (L+R)	2*	12	3,614,000	nd
	I4	2	3*	14	2,569,900	nd
	M3R	0	1*	6	2,380,100	nd
	PM4	0	1*	6	1,233,900	nd
	M3L	0	1*	5	813,500	nd
	PM5	0	1*	5	813,500	nd
	BM	0	1	2	503,700	nd
	MCL	1	0	0	0	nd

Figure S6, related to Figure 4. All I2 synapses observed by electron microscopy.

(A-D) Electron micrographs of all I2 synapses from two worms. Synapses can span many sections; only a single section is shown for each synapse. The synapse from I2 is in the center of each square micrograph, with the vesicles or presynaptic dense projection near the image center located inside the I2 neuron. In the caption below each square image, the number indicates the synapse ID and the cell names indicate the post-synaptic partners. Within each neuron within each worm, synapses are numbered from anterior to posterior. Underlined cell names indicate pharyngeal muscle.
(A) Electron micrographs of all I2L synapses identified in worm #1. All of the synapses were found in the anterior process of I2L, except when specified otherwise below each image.
(B) Electron micrographs of all I2L synapses identified in worm #4. All of the synapses were found in the posterior process of I2L.
(C) Electron micrographs of all I2R synapses identified in worm #1. All of the synapses were found in the anterior process of I2R, except when specified otherwise below each image.
(D) Electron micrographs of all I2R synapses identified in worm #4. All of the synapses were found in the posterior process of I2R.
(E) Table showing measurements for all I2 synapses identified in electron micrographs. The anterior neurites, soma and part of the posterior neurites were reconstructed from one adult hermaphrodite (worm #1), and the soma and posterior neurites were reconstructed from a second adult hermaphrodite (worm #4). The anterior synapses were confirmed by sparsely sampling a third worm (worm #5, data not shown). In the table, quantification of the anterior synapses was from worm #1, and quantification of the posterior synapses was from worm #4. The second column shows the number of synapses previously reported by Albertson and Thomson (1976), while the third column shows the number of synapses identified in this work. The fourth column shows the number of EM sections over which all of the synapses onto the recipient were distributed. Dense projection (DP) volumes and vesicle areas were calculated using the Measure feature of TrakEM2 [S1]. The listed DP volumes and vesicle areas are the sum of these values across all synapses with the specific partners indicated by the row in the table. * indicates that the synapse count included polyadic synapses in which the I2 synapse opposed more than one

cell. nd = not determined, BM = basement membrane. For post-synaptic partners NSML and NSMR, Albertson and Thomson (1976) did not distinguish whether the left or right NSM received the synapse from I2.

Figure S7:

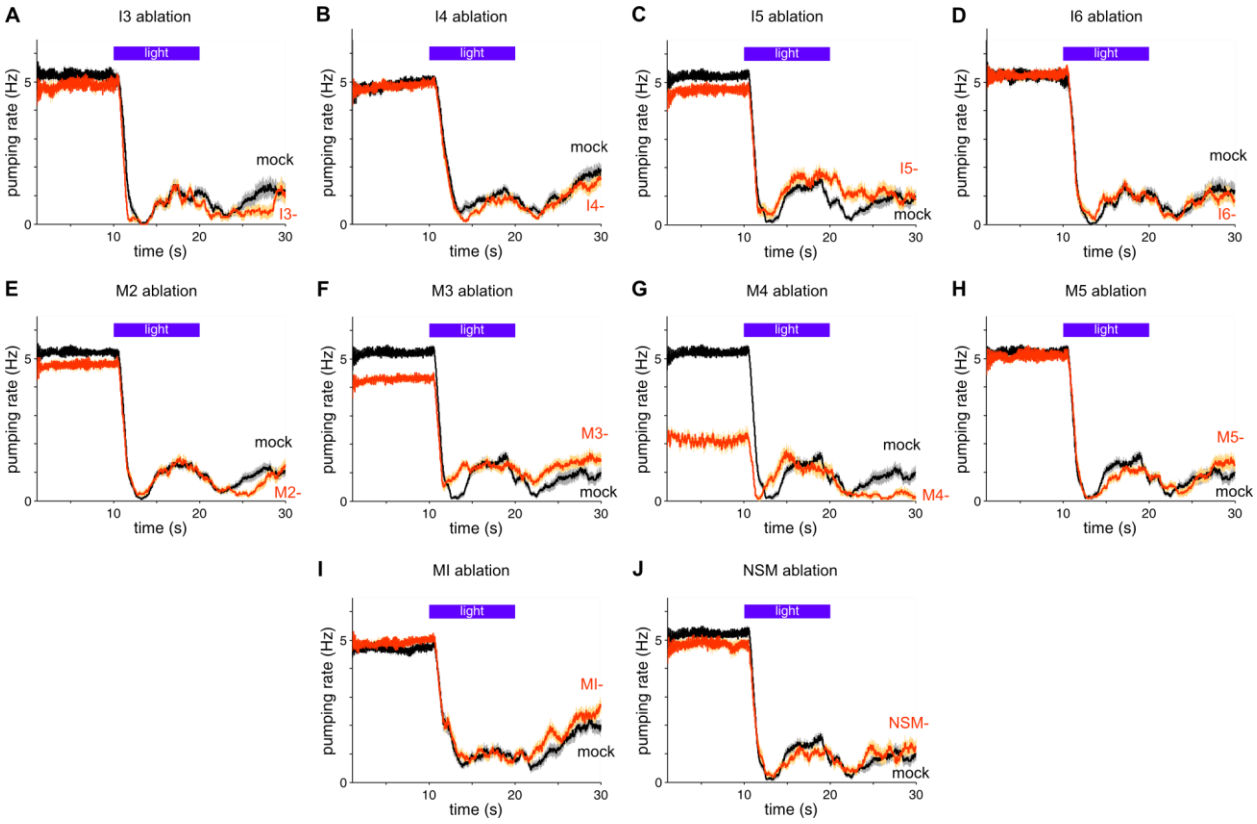

Figure S7, related to Figure 5. The effect of individual laser ablation of the remaining pharyngeal neurons on the pumping response to light.

(A) Ablation of the I3 neuron did not affect the pumping response to light. n = 18 trials, 6 worms.
(B) Ablation of the I4 neuron did not affect the pumping response to light. n = 30 trials, 12 worms. Reproduced from [S2].
(C) Ablation of the I5 neuron did not affect the pumping response to light. n = 26 trials, 9 worms.
(D) Ablation of the I6 neuron did not affect the pumping response to light. n = 27 trials, 10 worms.
(E) Ablation of the M2 neuron pair did not affect the pumping response to light. n = 35 trials, 11 worms.
(F) Ablation of the M3 neuron pair did not affect the acute response latency and caused a small but statistically significant defect in the acute response amplitude ($p < 0.001$, t-test). n = 37 trials, 13 worms.
(G) Ablation of the M4 neuron did not affect the acute or burst responses to light. n = 21 trials, 7 worms.
(H) Ablation of the M5 neuron did not affect the pumping response to light. n = 35 trials, 11 worms.

(I) Ablation of the MI neuron did not affect the pumping response to light. n = 34 trials, 13 worms.
(J) Ablation of the NSM neuron pair did not affect the pumping response to light. n = 23 trials, 8 worms.

Shading around traces indicate s.e.m.

SUPPLEMENTAL EXPERIMENTAL PROCEDURES

Strains

The following *C. elegans* strains were used (in order of mention):

N2 (wild-type)
MT21650 *nIs575[flp-15$_{prom}$::gcamp3; lin-15(+)]; lin-15(n765)*
MT21635 *nIs571[flp-15$_{prom}$::gcamp3; lin-15(+)]; lin-15(n765)*
MT21431 *nIs572[flp-15$_{prom}$::gcamp3; lin-15(+)]; lin-15(n765)*
MT21644 *nIs575; unc-31(u280); lin-15(n765)*
MT1212 *egl-19(n582)*
MT21639 *nIs575; egl-19(n582); lin-15(n765)*
CB55 *unc-2(e55)*
MT21652 *nIs575; unc-2(e55) lin-15(n765)*
JD21 *cca-1(ad1650)*
MT21787 *nIs575; cca-1(ad1650) lin-15(n765)*
CB251 *unc-36(e251)*
MT21637 *nIs571; unc-36(e251); lin-15(n765)*
VC550 *tag-180(ok779)*
MT21653 *tag-180(ok779); nIs575; lin-15(n765)*
VC12 *unc-77(gk9)*
MT21900 *nIs575; unc-77(gk9); lin-15(n765)*
VC9 *nca-2(gk5)*
MT21901 *nIs571; nca-2(gk5); lin-15(n765)*
CB540 *unc-68(e540)*
MT21651 *nIs575; unc-68(e540); lin-15(n765)*
JT73 *itr-1(sa73)*
MT21766 *nIs575; itr-1(sa73); lin-15(n765)*
MT21780 *nIs571; unc-36(e251); unc-2(e55) lin-15(n765)*
MT23567 *nIs575; egl-19(n582); unc-2(e55) lin-15(n765)*
MT23574 *nIs575; unc-2(e55) cca-1(ad1650) lin-15(n765)*
MT23569 *nIs571; unc-36(e251); egl-19(n582); lin-15(n765)*
MT23575 *nIs571; unc-36(e251); cca-1(ad1650) lin-15(n765)*
MT23578 *nIs575; egl-19(n582); cca-1(ad1650) lin-15(n765)*
MT23582 *nIs572; unc-36(e251); egl-19(n582); cca-1(ad1650) lin-15(n765)*
CB156 *unc-25(e156)*
CB933 *unc-17(e245)*
MT14984 *tph-1(n4622)*
CB1112 *cat-2(e1112)*
MT10548 *tdc-1(n3420)*
MT11374 *tbh-1(n3722)*
RB1821 *vglu-2(ok2356)*
FX03990 *vglu-3(tm3990)*
MT6308 *eat-4(ky5)*
MT6302 *eat-4(n2458)*

MT6318 *eat-4(n2474)*
DA819 *eat-4(ad819)*
DA572 *eat-4(ad572)*
MT20669 *eat-4(ok2233)*
IK883 *eat-4(ky5); njEx378[eat-4$_{prom}$::eat-4::gfp; ges-1$_{prom}$::gfp]*
MT21211 *eat-4(ky5); lin-15(n765); nIs529[flp-15$_{prom}$::eat-4 cDNA::gfp; lin-15(+) #1]*
MT21212 *eat-4(ky5); lin-15(n765); nIs530[flp-15$_{prom}$::eat-4 cDNA::gfp; lin-15(+) #2]*
MT21213 *eat-4(ky5); lin-15(n765); nIs531[flp-15$_{prom}$::eat-4 cDNA::gfp; lin-15(+) #3]*
MT21206 *eat-4(ky5); lin-15(n765); nIs524[gcy-10$_{prom}$::eat-4 cDNA::gfp; lin-15(+)]*
MT20722 *lite-1(ce314)*
MT20728 *eat-4(ky5); lite-1(ce314)*
MT21563 *eat-4(ky5); lite-1(ce314) lin-15(n765); nIs530*
VC3280 *F15A4.3(gk3259); flp-5(gk3123)*
VC20382 *flp-5(gk320541)*
VC2504 *flp-15(gk1186)*
MT15951 *nlp-3(n4897)*
VC1309 *nlp-8(ok1799)*
MT1541 *egl-3(n729)*
MT1218 *egl-3(n588)*
MT1071 *egl-21(n476)*
TU280 *unc-31(u280)*
MT22819 *eat-4(ky5); nIs569[flp-15$_{prom}$::csp-1b cDNA; ges-1$_{prom}$::gfp]*
MT6305 *glr-1(n2461)*
VM1390 *glr-2(ak10)*
VM1846 *glr-3(ak57)*
FX3239 *glr-4(tm3239)*
FX3506 *glr-5(tm3506)*
VM685 *glr-6(ak56)*
FX2877 *glr-7(tm2877)*
VC20465 *glr-8(gk283043)*
VM487 *nmr-1(ak4)*
VM6310 *nmr-2(ak7)*
DA1384 *avr-14(ad1302); glc-1(pk54)*
VC350 *glc-2(gk179)*
XA7400 *glc-3(ok321)*
JD31 *glc-4(ok212)*
DA1371 *avr-14(ad1302)*
FX1811 *mgl-1(tm1811)*
FX355 *mgl-2(tm355)*
FX1766 *mgl-3(tm1766)*
JD105 *avr-15(ad1051)*
MT22171 *avr-15(ad1051); lin-15(n765); nEx2149[myo-2$_{prom}$::avr-15A cDNA; lin-15(+)]*
OH4887 *otIs182[inx-18$_{prom}$::gfp]*
PS3504 *syIs54[ceh-2$_{prom}$::gfp, unc-119(+)]; unc-119(ed4)*
MT17641 *nIs264[gcy-10$_{prom}$::4xNLS::gfp, lin-15(+)]; lin-15(n765)*
MT17912 *nIs282[gcy-10$_{prom}$::4xNLS::gfp, lin-15(+)]; lin-15(n765)*

NL2334 *pkIs1273[gpa-16$_{prom}$::gfp]*
MT21198 *nEx1997[gpa-16$_{prom}$::gfp; unc-54$_{prom}$::rfp]*
MT23561 *nIs552[gcy-10$_{prom}$::chr2::yfp; lin-15(+)]; lite-1(ce314) gur-3(ok2245) lin-15(n765)*
MT21419 *nIs560[gcy-10$_{prom}$::enphr3::yfp; lin-15(+)]; lin-15(n765)*
MT23594 *nIs551[gcy-10$_{prom}$::chr2::yfp; lin-15(+)]; nIs711[flp-21$_{prom}$::gcamp3; lin-15(+)]; lite-1(ce314) gur-3(ok2245) lin-15(n765)*
MT23595 *nIs552; nIs711; lite-1(ce314) gur-3(ok2245) lin-15(n765)*

Molecular biology

We used the following primers to amplify DNA for generating transgenes by restriction enzyme cloning or PCR fusion. For cDNA, wild-type mixed-stage poly-A RNA was used as template.

flp-15$_{prom}$:	TGAACTTTCCTCATTTCCCCTTCGTTC, GACGAGGTGTATGTGGGAGACC
eat-4 cDNA:	ATGTCGTCATGGAACGAGGCTTG, CCACTGCTGATAATGCGGATTTTCC
myo-2$_{prom}$:	GTGTTGTGTATAGTGTACGAGAAAATGGAG, TTCTGTGTCTGACGATCGAGGGT
avr-15A cDNA:	ATGATAGGTCGATTGCGGAGAGG, CGTACTGATGGCCACACCGTATTG
gcy-10$_{prom}$ [S3]:	TGGGTACAACAATTTCTCATTCAAATT, TTTGAGCAGAAGGCCAATTATCGAAAAG
flp-21$_{prom}$ [S4]:	AACTAGGTCCAGTGACCGAAAGTG, CGTCTGAAAATGACTTTTTGGATTTTGGAG

Light-induced pumping response

This assay was conducted as previously described [S2]. Briefly, 1 day-old adult hermaphrodites were placed on a seeded NGM agar plate. Pumping was scored by eye using a stereo dissecting microscope set to 120x magnification and illuminated with a halogen transmitted light source (Zeiss Lumar and KL 2500 LCD, 3100 K). Custom Matlab software (available at www.wormweb.org) recorded the timing of pumps as indicated by manual key presses and controlled a shutter (via a Zeiss EMS-1 controller) that presented and removed mercury arc epi-illumination (HBO 100). We used a modified CFP filterset (Zeiss Lumar filter set 47 HE CFP

486047) to illuminate 436 ± 13 nm violet light at an intensity of 13 mW/mm^2. All experiments were done at 22.5 °C, unless specified otherwise. Data generated by real-time scoring was previously confirmed for wild-type and I2-ablated animals by video analysis [S2]. When assaying wild-type and mutant strains, each worm was assayed once. When assaying mock-ablated, ablated and ATR± worms, each worm was assayed 1-4 times.

Pharyngeal transport assay

To visualize the direction of flow in the pharynx for each pump, worms were fed either a 50% dilution of 1 µm polystyrene beads in M9 (Polysciences) or mineral oil. 1 day-old adults were placed with bacteria on an NGM agar pad on a coverslip and observed with a 20x objective on an inverted microscope (Zeiss Axiovert S100). Videos were recorded at 1000 fps using a high-speed camera (Photron Fastcam SA3), except that experiments with mineral oil were recorded at 86 fps using an EMCCD camera (Andor iXon+). 436 nm light (10 mW/mm^2; Till Photonics Polychrome V, 150 W Xenon bulb) was presented to the worm for 10 s. Videos were viewed and manually annotated, using custom Matlab software, for specific behavioral events: ingestion (beads being retained in the corpus after corpus relaxation), spitting (beads flowing out of the corpus), and pumping (movement of the grinder). In some cases, the worm moved out of the field-of-view of the camera, in which case those frames were annotated as "missing" and excluded from further analysis.

Behavioral statistics

Behavioral statistics were calculated as described previously [S2]. Briefly, the acute response latency is the time between the onset of light and the first missed pump. The first missed pump

is determined by identifying the first time interval between pumps that exceeds twice the pre-light pumping rate for that animal. The acute response amplitude is the rate of pumping in the first 3 s following the first missed pump divided by the pre-light pumping rate. The burst response amplitude is the rate of pumping in the last 5 s of light exposure divided by the pre-light pumping rate. Spitting rate was calculated as follows. First, for individual worms the spitting rate was calculated as the number of spits divided by the duration of light exposure, with "missing" frames excluded. Second, the spitting rate for a set of worms of a given condition was calculated as the weighted average of the individual worms' spitting rates, where the weight was determined as the fraction of the time that the worm was not missing from the field-of-view.

Laser ablations

We used a pulsed nitrogen laser to conduct laser microsurgery of individual pharyngeal neurons (Laser Science, Inc. VSL-337 attached to a Zeiss Axioplan microscope), as previously described [S5,S6]. Briefly, worms were immobilized by 10 mM sodium azide and mounted for viewing through a 100x oil objective. In general, ablations were performed on larvae of stage 1 or 2 (L1 or L2), with cells identified by nucleus location visualized with either Nomarski differential interference contrast optics or a cell-specific GFP reporter. Ablation of the M4 neuron was performed on larvae of stage 3 (L3), as the worms were more likely to grow to adulthood when ablated at this later stage. Ablations were confirmed the following day by appearance under Nomarski optics or by the loss of cell-specific fluorescence. On day 3 or 4, adults were assayed for their response to light.

Calcium imaging

We assayed the calcium response to light of the I2 neuron as previously described [S2]. Briefly, worms were immobilized using high friction [S7]. In our standard assay for I2, the worm was simultaneously imaged and stimulated with 26 mW/mm^2 485 nm blue light for 7 s, and videos were recorded at 15 fps. Frames of each video were aligned to minimize motion using the ImageJ plugin StackReg and analyzed for changes in fluorescence using manually drawn regions-of-interest (ROIs) and a custom Matlab program (available at www.wormweb.org). The latency of the calcium response of I2 was determined as the time from light onset to a fluorescence level greater than or equal to 20% above the baseline fluorescence level (i.e. 20% $\Delta F/F_0$). The amplitude of the calcium response of I2 was determined as the maximum GCaMP3 fluorescence observed during the duration of light stimulation/imaging. Outliers were excluded, such as if the I2 neuron was dark at baseline or did not respond to light exposure. For spatial analysis, we used a laser-scanning confocal microscope (Zeiss LSM 510) to selectively stimulate regions of the head with the 488 nm emission from a 25 mW argon laser. Videos were recorded at low resolution (128x128) so that a high frame rate could be sustained (5 fps). A 40x water objective was used. Worms were imaged for 2 s at 2% laser power, then an ROI was stimulated for 0.16 s (axon), 0.12 s (soma), or 0.62 s (dendrite) at 100% laser power, followed by imaging for 8 s. The duration of exposure for each ROI varied because the area of illumination varied, with each pixel in each ROI exposed for the same duration. For calcium imaging of MC, M4 and M2, the imaging conditions were the same as for I2 imaging except videos were recorded for a duration of 15 s. For the MC neurite, the posterior ventral neurite was analyzed only if it was separate from the M4 and M2 ventral neurites. The 485 nm light used for imaging also caused activation of ChR2. Since MC, M4 and M2 showed repeated calcium oscillations, a custom Matlab script analyzed the fluorescence changes and identified each likely calcium spike, which

was manually confirmed. The calcium peak amplitude was calculated as the difference between the fluorescence peak level and the lowest fluorescence level observed since the last peak. Changes in fluorescence due to changes in calcium could be distinguished from changes due to the motion caused by pumping by the fluorescence amplitude: pumping caused small transients superimposed on the larger transients caused by calcium changes. Only the first large fluorescence transient was included for analysis. For all calcium imaging assays, a single neuron of each class was assayed per animal, and each animal was assayed only once.

Optogenetic depolarization and hyperpolarization

Cultivation plates were seeded with 300 µl of OP50 *E. coli* mixed with 0.5 µl of 100 mM all-*trans* retinal (ATR+) or ethanol alone (ATR-) and incubated at room temperature for one day prior to placement of worms. Transgenic worms carrying channelrhodopsin (ChR2) [S8,S9] fused to yellow fluorescent protein (YFP) or halorhodopsin (eNpHR3) [S10] fused to YFP were cultivated on these plates in the dark from egg to adulthood. For ablation experiments, worms were cultivated with ATR± after ablation as L2 larvae. For behavioral assays, ChR2-expressing one day-old adults were illuminated after picking to plates lacking food, which retained a small amount of bacteria. eNpHR3-expressing worms were illuminated on the cultivation plate. We used a GFP filterset (Zeiss Lumar filter set 38 HE GFP 486038) to activate ChR2 with 470 ± 20 nm blue light at 1.5 mW/mm^2, and we used an RFP filterset (Zeiss Lumar filter set 43 HE RFP 486043) to activate eNpHR3 with 550 ± 13 nm green light at 10 mW/mm^2. To calculate the pumping rate during light exposure, the total pumps during light exposure were divided by the time interval of light exposure (10 s). For optogenetics with calcium imaging, see the "Calcium imaging" section above.

Expression analysis

To observe gene expression of *njEx378[eat-4$_{prom}$::eat-4::gfp]* in I2, images were recorded using a light microscope (Zeiss Axioskop 2) and a CCD camera (Hamamatsu ORCA-ER).

Electron microscopy

Adult N2 worms were loaded into a Type A carrier coated with 1-hexadecene and filled with a slurry of OP50 *E. coli*, then covered with a Type B carrier [S11]. The sandwich was placed into the specimen holder and frozen using a high pressure freezer (Abra HPM010). Samples were substituted with 1% OsO_4, 0.2% uranyl acetate in 95% acetone::5% methanol at -90 °C for 110 h, warmed to -20 °C over 14 h, held at -20 °C for 16 h and warmed to 0 °C over 3.3 h (RMC FS-2500) [S12]. Samples were washed three times with acetone at 0 °C and three times at room temperature before stepwise infiltrated with Eponate 12 resin (Ted Pella) and polymerized at 65 °C. Individually embedded worms were thin-sectioned and imaged with a transmission electron microscope (JEOL JEM-1200 ExII) and CCD camera (AMT XR1241) at multiple magnifications (5,000x, 10,000x, 40,000x). Section thickness varied between 40-50 nm, with the 5,000x magnification images spanning a 30 x 30 µm area. Images were cropped to remove captions, automatically aligned using TrakEM2 [S1] in Fiji, and then the alignment was manually corrected. Cells in the anterior pharynx were manually traced. Synapses from the I2 neurons were annotated if more than two vesicles were present near the membrane or a clearly visible dense projection was present in the absence of vesicles. Dense projections were manually annotated, and their volumes were quantified using the Measure feature of TrakEM2. Synaptic vesicles were manually annotated, and their areas were quantified using the Measure feature of

TrakEM2. Synapse size was calculated as the sum of the dense projection volume and volumes of synaptic vesicles, using the average vesicle diameter we observed, 30 nm; this method was applied uniformly whether the synaptic output was to a single partner or multiple partners (polyadic).

Supplemental References

[S1] Cardona, A., Saalfeld, S., Schindelin, J., Arganda-Carreras, I., Preibisch, S., Longair, M., Tomancak, P., Hartenstein, V. & Douglas, R. J. (2012). TrakEM2 software for neural circuit reconstruction. PLoS One *7*, e38011.

[S2] Bhatla, N. & Horvitz, H. R. (2015). Light and hydrogen peroxide inhibit *C. elegans* feeding through gustatory receptor orthologs and pharyngeal neurons. Neuron *85*, 804-818.

[S3] Yu, S., Avery, L., Baude, E. & Garbers, D. L. (1997). Guanylyl cyclase expression in specific sensory neurons: A new family of chemosensory receptors. Proceedings of the National Academy of Sciences *94*, 3384-3387.

[S4] Rogers, C., Reale, V., Kim, K., Chatwin, H., Li, C., Evans, P. & de Bono, M. (2003). Inhibiton of *Caenorhabditis elegans* social feeding by FMRFamide-related peptide activation of NPR-1. Nature Neuroscience *6*, 1178-1185.

[S5] Bargmann, C. I. & Avery, L. (1995). Laser killing of cells in *Caenorhabditis elegans*. In Methods in Cell Biology, Epstein, H. F. & Shakes, D. C., ed. (San Diego: Academic Press), pp. 225-250.

[S6] Fang-Yen, C., Gabel, C. V., Samuel, A. D. T., Bargmann, C. I. & Avery, L. (2012). Laser Microsurgery in *Caenorhabditis elegans*. In *Caenorhabditis elegans*: Cell Biology and Physiology, Rothman, J. H. & Singson, A., ed. (Boston: Academic Press), pp. 177-206.

[S7] Kim, E., Sun, L., Gabel, C. V. & Fang-Yen, C. (2013). Long-term imaging of *Caenorhabditis elegans* using nanoparticle-mediated immobilization. PLoS One *8*, e53419.

[S8] Boyden, E. S., Zhang, F., Bamberg, E., Nagel, G. & Deisseroth, K. (2005). Millisecond-timescale, genetically targeted optical control of neural activity. Nature Neuroscience *8*, 1263-1268.

[S9] Nagel, G., Brauner, M., Liewald, J. F., Adeishvili, N., Bamberg, E. & Gottschalk, A. (2005). Light activation of Channelrhodopsin-2 in excitable cells of *Caenorhabditis elegans* triggers rapid behavioral responses. Current Biology *15*, 2279-2284.

[S10] Gradinaru, V., Zhang, F., Ramakrishnan, C., Mattis, J., Prakash, R., Diester, I., Goshen, I., Thompson, K. R. & Deisseroth, K. (2010). Molecular and cellular approaches for

diversifying and extending optogenetics. Cell *141*, 154-165.

[S11] Hall, D. H., Hartweig, E. & Nguyen, K. C. Q. (2012). Modern Electron Microscopy Methods for *C. elegans*. In Methods in Cell Biology, Rothman, J. H. & Singson, A., ed. (San Diego: Academic Press), pp. 93-149.

[S12] Fetter, R. (2013). High pressure freeze of embryos and L1s, Available at http://www.wormatlas.org/EMmethods/Highpressurefreezeembryo.htm.